Biosensors and Bioelectronics 60 (2014) 137–142

Contents lists available at ScienceDirect

Biosensors and Bioelectronics

journal homepage: www.elsevier.com/locate/bios

Sensitive electrochemical microbial biosensor for *p*-nitrophenylorganophosphates based on electrode modified with cell surface-displayed organophosphorus hydrolase and ordered mesopore carbons

Xiangjiang Tang [a,1], Tingting Zhang [a,b,1], Bo Liang [a], Dongfei Han [a], Lingxing Zeng [c], Cheng Zheng [c], Tie Li [b], Mingdeng Wei [c], Aihua Liu [a,*]

[a] Laboratory for Biosensing, Qingdao Institute of Bioenergy & Bioprocess Technology, and Key Laboratory of Bioenergy, Chinese Academy of Sciences, 189 Songling Road, Qingdao 266101, China, and University of Chinese Academy of Sciences, 19A Yuquan Road, Beijing 100049, China
[b] College of Chemistry and Chemical Engineering, Ocean University of China, 238 Songling Road, Qingdao 266100, China
[c] Institute of Advanced Energy Materials, Fuzhou University, Fuzhou, Fujian 350002, China

ARTICLE INFO

Article history:
Received 14 January 2014
Received in revised form
1 April 2014
Accepted 1 April 2014
Available online 8 April 2014

Keywords:
Bacterial surface display
Organophosphorus hydrolase
p-nitrophenyl organophosphates
Ordered mesoporous carbons
Electrochemical microbial biosensor
Amperometric detection

ABSTRACT

A novel electrochemical microbial biosensor for the rapid monitoring of *p*-nitrophenyl-substituted organophosphates (OPs) compounds based on glass carbon electrode (GCE) modified with both ordered mesopore carbons (OMCs) and cell surface-expressed organophosphorus hydrolase (OPH) (OPH-bacteria/OMCs/GCE) was described in this paper. The genetically engineered *Escherichia coli* strain surface displayed mutant OPH (S5) with improved enzyme activity and favorable stability was constructed using a newly identified N-terminal of ice nucleation protein as an anchoring motif, which can be used directly without further time-consuming enzyme-extraction and purification, thereafter greatly improved the stability of the enzyme. Compared to OPH-bacteria modified GCE (OPH-bacteria/GCE), the OPH-bacteria/OMCs/GCE not only significantly enhanced the current response but also reduced the oxidation overpotential towards oxidizable *p*-nitrophenol (*p*-NP), which was the hydrolysate of *p*-nitrophenyl-substituted OPs. Under the optimized experimental conditions, at +0.84 V (vs. SCE), the current–time curve was performed with varying OPs concentration. The current response was linear with paraoxon concentration within 0.05–25 μM. Similarly, linear range of 0.05–25 μM was found for parathion, and 0.08–30 μM for methyl parathion. The low limits of detection were evaluated to be 9.0 nM for paraoxon, 10 nM for parathion and 15 nM for methyl parathion ($S/N=3$). Thus, a highly specific, sensitive and rapid microbial biosensor was established, which holds great promise for on-site detection of trace *p*-nitrophenyl-substituted OPs.

1. Introduction

Organophosphates (OPs) represent one kind of broadly existing acute toxicity species, which are found widely as contaminants (Chough et al., 2002; J and Králové, 2002; Wang et al., 2002; Zhang et al., 2014b). The chemical structures of some common OPs are listed (Supplementary material, Fig. S1). It is estimated that over 1500 kinds of OP compounds have been synthesized during the past 20th century, which are commercially used as pesticides and chemical warfare agents (Brown and Brix, 1998; Eskenazi et al., 1999; Rahimi and Abdollahi, 2007; Schoning et al., 2003). There are stringent restrictive regulations worldwide about OPs especially for *p*-nitrophenyl OPs (e.g. paraoxon, parathion and methyl parathion, etc.), which belong to highest poisonous OPs. For example, paraoxon is used as typical insecticide with a human oral lethal dose of 5 mg/kg (Deo et al., 2005a; Lei et al., 2005; Minton and Murray, 1988; Wang et al., 2003). Parathion would convert into paraoxon through a series of photolysis and metabolic oxidation process (Lei et al., 2007; Lukaszewicz-Hussain, 2010; Mulchandani et al., 2006). So it is highly desirable to ensure that these *p*-nitrophenyl OPs are not present over hazardous levels in food, ground water and soil. Currently, conventional laboratory-based analytical methods for determining *p*-nitrophenyl OPs include primarily gas and liquid chromatography (Pinto et al., 1995), liquid- and thin-layer chromatography (Bravo et al., 2002) and different types of spectroscopy (Mathew et al., 2007; Tang et al., 2014), capillary electrophoresis (Chen and Fung, 2010) and flow injection analysis (Mulchandani et al., 2001; Wang et al., 2003), etc. However, the shortages of these

* Corresponding author. Tel: +86 532 8066 2758; fax: +86 532 8066 2778.
E-mail address: liuah@qibebt.ac.cn (A. Liu).
[1] These two authors contributed equally to this work.

http://dx.doi.org/10.1016/j.bios.2014.04.001
0956-5663/

analytical technologies such as the time-consuming procedure in sample preparation, the large-scale and expensive instruments and high cost in instrumental maintenance indicated that those technologies were not suitable for on-site test. Accordingly, there are growing demands for field-deployable devices for reliable monitoring of *p*-nitrophenyl OPs.

Organophosphorus hydrolase (EC 3.1.8.1, OPH) can hydrolyze effectively a broad range of organophosphorus esters, which has been widely used as an important component of OPs enzyme biosensors (Ashok Mulchandani, 2011). *p*-nitrophenyl OPs such as parathion methyl parathion and paraoxon can be catalyzed by OPH to form *p*-nitrophenol (*p*-NP), and *p*-NP shows optical absorption at 410 nm approximately. At present, several types of OPH-based biosensors have been introduced, including potentiometric, amperometric or optical devices (Choi et al., 2010; Du et al., 2010; Lee et al., 2010; Tang et al., 2014). Other enzymatic devices based on the inhibition of acetylcholine esterase (AChE) have been widely used for the detection of OPs (Chen et al., 2011; Soltaninejad and Abdollahi, 2009). Generally speaking, although AchE-based biosensors were more sensitive than OPH-based biosensors, they are cumbersome in operating procedures, lots of jamming signals and poor specificity, which only provided the total quantity of a series of toxic inhibitors (Mulchandani et al., 2001).

Microbial surface display could eliminate onerous purification of OPH by fusing it with appropriate anchoring motifs such as outer membrane protein (OmpA) (Karami et al., 2014), ice nucleation protein (INP) (Shimazu et al., 2003) and a-agglutinin (Schofield et al., 2007). However, the OPH activity of surface displayed strains reported earlier is relatively low, which cannot meet the need for sensitive OPH biosensors (Deo et al., 2005b). Therefore, mutated OPH (S5) with improved enzyme activity was displayed on the surface of *E. coli* using INP display system in our laboratory (Tang et al., 2014). The resultant whole cell exhibited excellent OPH activity and stability (Tang et al., 2014), which could provide the ideal bacterial candidate for biosensing of OPs.

In the past decades, electrochemical methods were regarded as high sensitivity, good reproducibility and minimal space and low-cost instrumentation methods, attracting more and more attention for on-site monitoring of *p*-nitrophenyl OPs. Ordered mesopore carbons (OMCs) were popularly used in many aspects due to their outstanding physico-chemical properties (Ndamanisha and Guo, 2012). OMCs with uniform porous channels, large surface area and well-defined pore topology made it the perfect carrier of cell and thus enhance the stability of the enzyme. The oxygen-containing functional groups on the surface of OMCs can combine with the enzyme, and accordingly, which is capable of letting the activity center of enzyme-bacteria exposed to the substrate, and thus retain the enzyme activity (Laothanachareon et al., 2008). Additionally, the edge plane-like defective site on the surface of OMCs can provide a great deal of favorable sites to transmit electrons of electroactive substances (Ndamanisha and Guo, 2012).

In this paper, OMCs were proved to be a satisfactory material for immobilizing cell-surface-expressed OPH in developing novel electrochemical biosensor for *p*-nitrophenyl OPs. The OPH-bacteria with high activity and stability was used directly without further laborous enzyme-extraction and purification, which greatly improved the stability of the enzyme. By detection of the oxidation current of *p*-NP which was the hydrolysis product of *p*-nitrophenyl-substituted OPs, the rapid monitoring of *p*-nitrophenyl OPs was realized. Paraoxon was used as the analyte to systematically study the electrochemical behavior of *p*-nitrophenyl OPs at OPH-bacteria/OMCs/GCE and optimized the experimental conditions. Thus, a highly specific, sensitive and rapid microbial biosensor for trace detection of *p*-nitrophenyl OPs was established. This biosensor would be well-suited for meeting the challenges of on-site determination.

2. Materials and methods

2.1. Chemicals and reagents

Paraoxon, parathion and methyl parathion were purchased from Sinopharm Chemical Reagent Corporation and used without further purification. The 20 mM stock OP solutions were prepared with methanol and water (1:5) and stored in darkness to avoid photolysis. The experimental solutions should be prepared immediately before use. For safety, these OP compounds should be handled in the fumehood. Direct contact and inhalation should be avoided by taking appropriate security precautions. Nafion (perfluorinated ion-exchange resin, 5 wt% solution in a mixture of lower aliphatic alcohols and water) were purchased from Aldrich Corporation. 0.1 M phosphate buffer saline (PBS, pH 7.4) was served as the supporting electrolyte. All other chemicals were of the highest grade and all the solutions were prepared with ultrapure water. OMCs were synthesized according to the procedure in our published paper, which exhibited large surface area and uniform mesopore channel structure with an average pore diameter of approximately 3.9 nm (Zhang et al., 2013).

2.2. Bacterial strains and plasmids, growth of bacteria-displayed OPH

The construction of expression vector pTInaPb-N/Oph has been completed in our previous study (Tang et al., 2014). To obtain the cells surface displayed mutated OPH (S5) for construction of biosensor in the present study, the growth of bacteria was conducted according to the procedures reported earlier (Tang et al., 2014). Briefly, *E. coli* strain BL21 (DE3) was used as the host cell for the expression of recombinant protein INP-OPH. Cells bearing the expressing plasmid pTInaPb-N/OPH were grown in LB media with 50 mg/L kanamycin at 37 °C. Fusion proteins were induced with isopropyl-*β*-D-thiogalactoside (IPTG) at final concentration of 0.1 mM at 25 °C for 8 h. Then cells were harvested and resuspended in 75 mM Tris-HCl buffer with 50 μM $CoCl_2$ (pH 8.0). The procedure for cell fractionation and enzyme activity assay has been described before (Tang et al., 2014).

2.3. Electrode fabrication

The bare GCE (3 mm in diameter) was polished successively with 0.3 and 0.05 μm alumina slurry and sonicated for about 3 min. Nafion–OMCs composite was prepared by dispersing 2.0 mg OMCs powder into 1.0 mL Nafion (0.05 wt%) which was diluted from 5 wt% Nafion and sonicated to obtain a homogeneous dispersion. A 10 μL aliquot of this Nafion–OMCs composite was cast onto the cleaned bare GCE. Next, 10 μL of OPH-bacteria aqueous dispersion was added to the modified GCE as to OPH-bacteria/OMCs/GCE and dried overnight at 4 °C. Before use, 4.0 μL of Nafion (0.05 wt%) was syringed onto the surface of modified electrode. The Nafion/bacteria-OPH/GCE was prepared for comparison. The microbial electrode was kept in a refrigerator (at 4 °C) when not in use.

2.4. Apparatus and methods

The electrochemical measurements were performed on CHI 660D electrochemical workstation (Chenhua Co., Shanghai, China) with a conventional three-electrode system using bare GCE or modified GCE as working electrode, platinum wire as auxiliary electrode and saturated calomel electrode (SCE) as reference electrode, respectively. All potentials in this paper were recorded versus this reference. PB-10 pH meter (Sartorius AG, Germany) was applied for pH adjustment. All electrochemical measurements

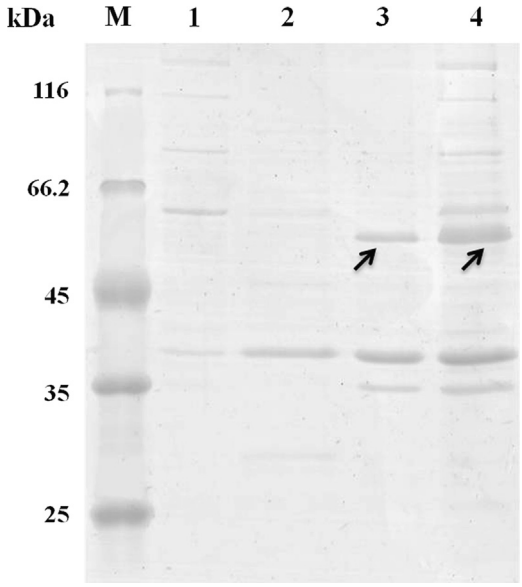

Fig. 1. SDS-PAGE analysis of INP–OPH fusion in different cellular fractions. Lane M, protein marker. Lanes 1–4, *E. coli* cells harboring pTInaPb-N/Oph: lane 1, cytoplasmic fraction; lane 2, inner membrane fraction; lane 3, outer membrane fraction; lane 4, total cell lysate.

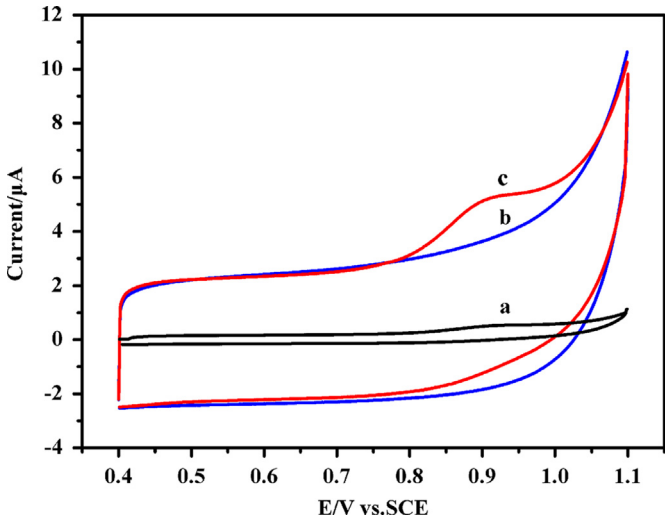

Fig. 2. CVs of (a) OPH-bacteria/GCE in 10 μM paraoxon buffered with 0.1 M PBS (pH 7.4), (b) OPH-bacteria/OMCs/GCE in blank PBS (pH 7.4), and (c) OPH-bacteria/OMCs/GCE in 10 μM paraoxon buffered with 0.1 M PBS (pH 7.4).

were performed at room temperature (~23 °C). Differential pulse voltammetry conditions were below: equilibration time, 2 s; potential amplitude, 50 mV; pulse period: 0.5 s; step height, 4 mV; frequency, 60 Hz.

3. Results and discussion

3.1. Preparation of bacteria-OPH

The production and transportation of OPH mediated by the INP bacteria surface display system were measured by SDS-PAGE analysis, which revealed that the majority of OPH–INP fusion proteins were located on the outer membrane fraction of cells (Fig. 1). The enzyme activity was determined by the spectrophotometric method using paraoxon as the substrate. According to the results, the OPH activity of whole cells was 12.44 U/mg cells (dry weight). Here unit activity was defined as the amount of enzyme necessary for the production of 1 μmol *p*-NP per minute per mg whole cells. The thermostability assay carried out in our previous study showed that the activity of cell surface displayed OPH remained the same level of its initial enzyme activity over one month period at room temperature (Tang et al., 2014). In previous study, OPH was displayed on the surface of cells based on several different microbial display systems (Fukuda et al., 2010; Karami et al., 2014; Takayama et al., 2011). However, the relatively low whole cell OPH activity was the bottleneck to improve OPs biosensor's performance (Liu et al., 2013). In our study, the cell surface displayed OPH exhibited much higher enzyme activity and better storage stability than other related research reported before (Karami et al., 2014; Liu et al., 2013; Schofield et al., 2007), which has demonstrated that the whole-cell biocatalyst was the most promising candidate to be used in the field of OPH biosensor.

3.2. Electrochemical behavior of paraoxon at OPH-bacteria/GCE and OPH-bacteria/OMCs/GCE

The general reaction mechanism for the OPH catalyzed the hydrolysis of *p*-nitrophenyl OPs was widely reported (Karami et al., 2014; Tang et al., 2014). The *p*-nitrophenyl OPs were hydrolyzed to generate *p*-nitrophenol (*p*-NP),) which could be electrochemically oxidized and the reaction mechanism was introduced in detail in our published paper (Zhang et al., 2014a). The cyclic voltammograms (CVs) of 10 μM paraoxon in 0.1 M PBS (pH 7.4) buffer at different modified electrodes are shown (Fig. 2). At OPH-bacteria/GCE, a weak and broad oxidation peak was observed at 0.906 V, which was the oxidation of the hydrolysis product (*p*-NP) (Fig. 2, curve a). Meanwhile, an enhanced *p*-NP oxidation peak was exhibited at 0.895 V at OPH-bacteria/OMCs/GCE (Fig. 2, curve c). There was no peak in the absence of substrate at OPH-bacteria/OMCs/GCE in 0.1 M PBS (pH 7.4) buffer (Fig. 2, curve b). The electrochemical oxidation of *p*-NP, the hydrolysis product of paraoxon by OPH, was typically totally irreversible. Unfortunately, cyclic voltammetry (CV) was not sensitive enough to detect paraoxon because the peak was not apparent. The electrochemical behavior of paraoxon was further systematically studied by differential pulse voltammetry (DPV) which has a better resolution and signal-to-noise ratio compared with CV. The anodic differential pulse voltammograms (DPVs) of paraoxon at OPH-bacteria/GCE and OPH-bacteria/OMCs/GCE were recorded in 0.1 M PBS (pH 7.4) buffer (Fig. 3). A weak oxidation peak was observed at 0.867 V for 10 μM paraoxon at OPH-bacteria/GCE (Fig. 3, curve a). The DPVs of different concentrations of paraoxon at OPH-bacteria/OMCs/GCE were recorded. The oxidation peak current at 0.856 V increased as paraoxon concentration increased from 0 to 10 μM. By comparing curves a and d in Fig. 3, it was very clear that the modification of the electrode with OMCs not only significantly enhanced the current response of 5 μM paraoxon but also performed certain catalysis and reduced the oxidation overpotential to some extent. It might be attributed to the plenty of edge plane-like defects on the surface of OMCs which would provide lots of favorable sites for electron transfer and oxygen-containing functional groups on the surface of OMCs, which can form hydrogen bonds with the OH groups of *p*-NP to weaken the bond energy of Ar-OH and facilitate the oxidation of *p*-NP. Moreover, the large surface area, arranged mono-dispersed mesopore and the silicon dioxide residual in wall of hole might preconcentrate paraoxon intensely (Ndamanisha and Guo, 2012; Zhang et al., 2013). In the following section, the experimental conditions such as cell loading, buffer pH, operating potential were optimized to improve the detection sensitivity of OPs at OPH-bacteria/OMCs/GCE.

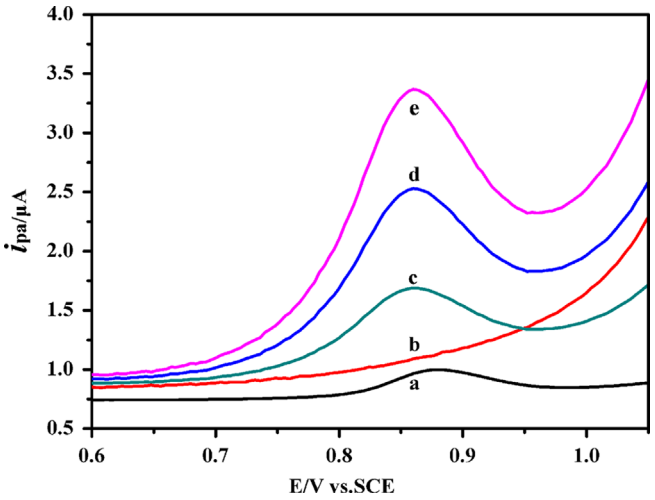

Fig. 3. Differential pulse voltammograms (DPVs) of 5.0 μM paraoxon in 0.1 M PBS (pH 7.4) at OPH-bacteria/GCE (a) and the DPVs of OPH-bacteria/OMCs/GCE with different concentrations of paraoxon: 0 μM (b), 2.5 μM (c), 5.0 μM (d) 10 μM (e). Experimental conditions: equilibration time: 2 s; potential amplitude: 50 mV; pulse period: 0.5 s; step height: 4 mV; and frequency: 60 Hz.

3.3. Optimization of experimental conditions

3.3.1. Effect of cell loading

As expected, the loading of OPH-bacteria with different dilution ratios had a profound effect upon the performance of OPH-bacteria/OMCs/GCE in the presence of 5 μM paraoxon (Fig. 4). As dilution ratio increased, the current response climbed up first and reached to the maximum at dilution ratio of 1:5 and then declined significantly (Fig. 4B). Interestingly, the as-prepared OPH-bacteria (without dilution) modified electrode did not give the maximal current response. It is definite that the thickness of the enzyme membrane decreased with the increasing of the dilution ratio of OPH-bacteria. When the as-prepared OPH-bacteria solution was used, the thickness of the resulted enzyme membrane may be so thick that probably blocks the electron transfer between the substrate and electrode surface (Li et al., 2012, 2013). As well, the excessive dilution may restrict the effective quantity of enzyme and performed a lower biocatalytic activity. Overall, the sensitivity of the OPH-bacteria/OMCs/GCE corresponded to a tradeoff between higher biocatalytic activity and electron transport limitations. Thus, 10 μL surface loading of the 1:5 diluted ratio OPH-bacteria were selected for further studies.

3.3.2. Effect of pH

As proton participates in the electrode reaction and the OPH-bacteria has an optimum acidity to obtain high enzyme activity and stability (Tang et al., 2014; Zhang et al., 2014a), the pH of the buffer has a remarkable influence on the performance of OPH-bacteria/OMCs/GCE and here the oxidation peak of the hydrolysis product (*p*-NP) was evaluated by DPV (Supplementary material, Fig. S2A). The increase of buffer pH from 6.0 to 9.0 resulted in a slight enhancement of the current signal at first, and then a sharp increase was observed. As buffer pH increased from 6.0 to 9.0, the current response climbed up first and reached to the maximum at pH 7.4, and then declined significantly (Supplementary material, Fig. S2B). So PBS buffer with pH 7.4 was selected for the subsequent experiments to obtain the high sensitivity.

3.3.3. Effect of operating potential of current–time curves

The performance of OPH-bacteria/OMCs/GCE towards paraoxon was described by current–time curves in the subsequent experiments,

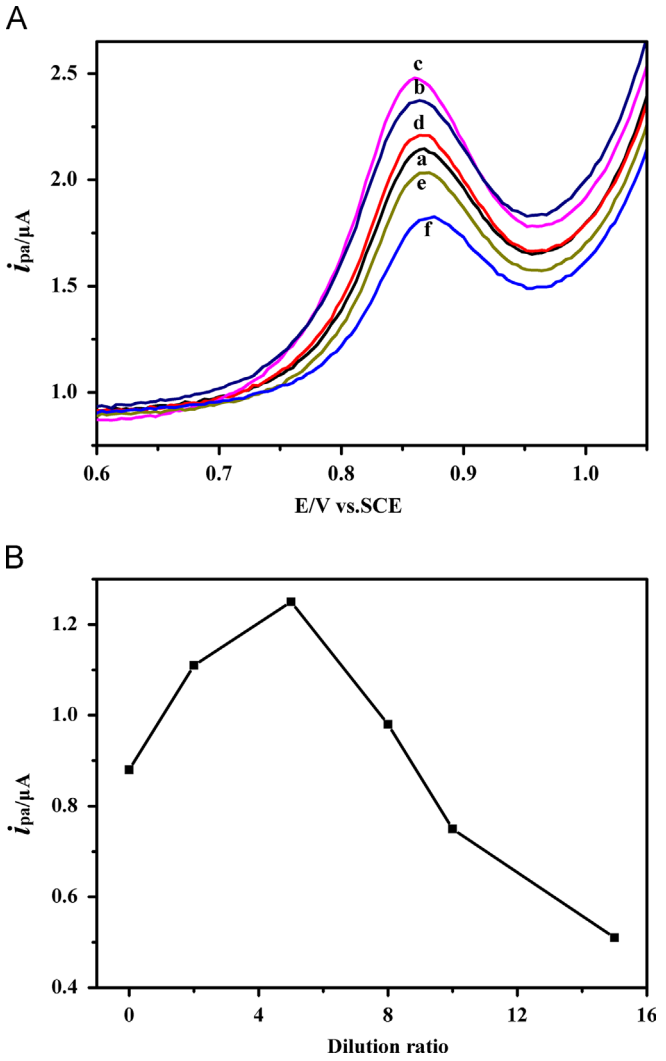

Fig. 4. (A), DPVs of 5 μM paraoxon at OPH-bacteria/OMCs/GCE (c) in 0.1 M PBS (pH 7.4) modified with 10 μL OPH-bacteria varying different dilution ration of the original OPH-bacteria. Dilution ration: (a), no dilution; (b), 1:2; (c), 1:5; (d), 1:8; (e), 1:10; and (f), 1:15. (B), the relationship between i_{pa} and different dilution ration of the original OPH-bacteria Experimental conditions: equilibration time, 2 s; potential amplitude, 50 mV; pulse period: 0.5 s; step height, 4 mV; frequency, 60 Hz.

it is important to find the proper operating potential to obtain the strong signal. The current–time curve of OPH-bacteria/OMCs/GCE at different operating potentials with increasing concentration of paraoxon in 1 μM steps is shown (Supplementary material, Fig. S3A). To obtain the reliable result, it was handled for five times and the average value was calculated. As the operating potential increased from +0.78 V to +0.88 V, the current signal of 1 μM paraoxon was enhanced because the oxidation of the substrate was more and more complete. After the operating potential 0.84 V, the current signal increased quite slowly (Supplementary material, Fig. S3B). So the subsequent amperometric detections were carried out at a potential of +0.84 V, which offered the higher signal-to-noise ratio and the major signal. This working potential is similar to those reported in previous studies.

3.4. Analytical characteristics of microbial sensor

Under the above optimal experimental conditions, the current–time curve at OPH-bacteria/OMCs/GCE was obtained by using amperometry at an operating potential of 0.84 V (Fig. 5). The oxidation current increased after addition of paraoxon and

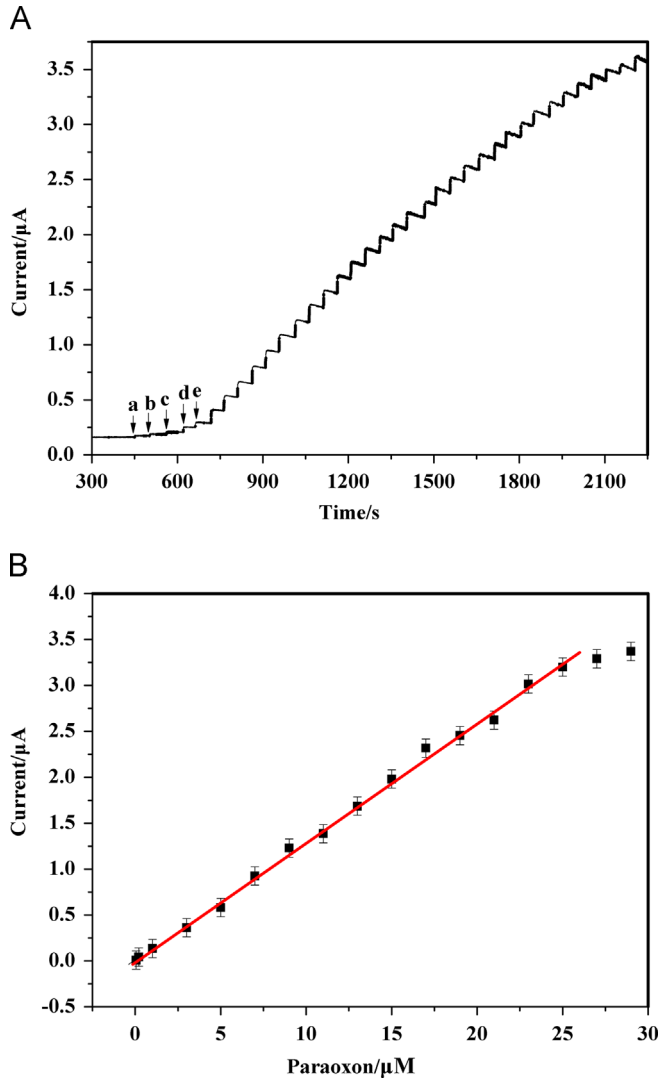

Fig. 5. (A) Current–time curve obtained at the OPH-bacteria/OMCs/GCE on the successive addition of paraoxon in 0.1 M PBS (pH 7.4). (a), 0.05 μM; (b), 0.10 μM; (c), 0.2 μM; (d), 0.5 μM; and (e), 1.0 μM; and with increasing concentration of paraoxon in 1 μM step afterwards. Experimental conditions: operating potential, 0.84 V; stirring rate, 300 rpm. (B) Typical calibration graph of the biosensor for paraoxon.

reached at 95% steady-state value within 5 s (Fig. 5A) indicating that the reaction on the modified electrode was quite rapid. However, a plateau appeared when paraoxon was higher than 25 μM, which were probably originating from the saturated adsorption of substrate at the surface of OPH-bacteria/OMCs/GCE. The calibration curve of paraoxon was shown in Fig. 5B. The current response linearly increased with the increasing concentration of paraoxon over the concentration of 0.05–25 μM. The linear regression equation is i_{pa} (paraoxon)=0.0090+0.1291Conc, with a correlation coefficient R=0.9978. The limit of detection (LOD) is 9.0 nM paraoxon (S/N=3). Some other kinds of OPs were also measured at OPH-bacteria/OMCs/GCE and the results were summarized in Table 1. Parathion and methyl parathion which belong to *p*-nitrophenyl OPs can be detected sensitively. The LOD of parathion and methyl parathion was 10.0 nM and 15.0 nM, respectively (Table 1). Those OPs such as phoxim, chlorpyrifos and dimethoate that could not be hydrolyzed to *p*-NP by OPH-bacteria, exhibit no responses at OPH-bacteria/OMCs/GCE (Table 1). The performance of various sensors for the detection of *p*-nitrophenyl OPs was listed (Supplementary material, Table S1). Obviously, the

Table 1
The linear range and the limit of detections of some typical OPs at OPH-bacteria/OMCs/GCE.

OPs	Linear range (μM)	LOD (nM)
Paraoxon	0.05–25	9.0
Parathion	0.05–25	10.0
Methyl parathion	0.08–30	15.0
Phoxim	ND	–
Chlorpyrifos	ND	–
Dimethoate	ND	–

ND, not detectable. Current–time curve conditions: operating potential: 0.84 V, stirring rate: 300 rpm.

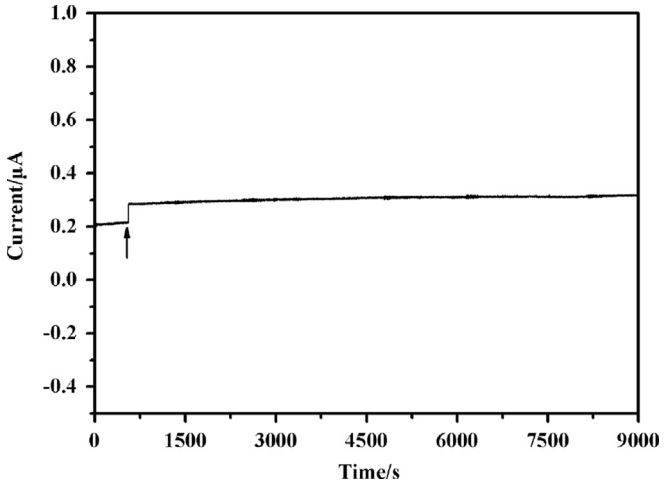

Fig. 6. Operating stability of the OPH-bacteria/OMCs/GCE measured by injecting 1 μM paraoxon in 0.1 M PBS (pH 7.4) buffer and operating for about 8000 s. Experimental conditions: operating potential, 0.84 V; stirring rate, 300 rpm.

OPH-bacteria/OMCs/GCE in this study showed wider dynamic detection ranges and corresponding lower detection limits. Compared to optical and spectrophotometric OPH-bacteria sensor, the OPH-bacteria/OMCs/GCE in this work was more suitable for on-site detection with higher sensitivity. Compared to purified OPH based electrochemical sensor, the OPH-bacteria in this work with high activity and stability was used directly without further time-consuming enzyme-extraction and purification, which greatly improved the stability of the enzyme and had high sensitivity. Compared to the direct detection without enzyme, the OPH-bacteria/OMCs/GCE was highly specific towards *p*-nitrophenyl OPs. In addition, the preparation of OPH-bacteria/OMCs/GCE was pretty simple and exhibited wider dynamic detection ranges and corresponding lower detection limits which were applicable for on-site determination of *p*-nitrophenyl OPs.

3.5. Stability of OPH-bacteria/OMCs/GCE

A consecutive current–time measurement was carried out to test the operational stability of OPH-bacteria/OMCs/GCE (Fig. 6). There were no apparent ups and downs of the current–time curve after operating for about 8000 s with 1 μM paraoxon in 0.1 M PBS (pH 7.4) buffer, indicating that the OPH-bacteria/OMCs/GCE exhibited good operational stability. The long-term stability of the sensor was also evaluated. The current response of the modified electrode was measured daily in 0.1 M PBS (pH 7.4) buffer in the presence of 1 μM paraoxon. The biosensor was stored under 4 °C when it was not in use. During one-month test, the current signals of the OPH-bacteria/OMCs/GCE still remained 70% of initial

Table 2
Determination of *p*-nitrophenyl OPs in real samples.

p-nitrophenyl OPs	Tap water	Seawater	Sewage
Content (μM)	0.00	0.00	1.05
Added paraoxon (μM)	5.00	5.00	5.00
Found paraoxon (μM)	4.89	4.86	6.22
RSD (% $n=6$)	2.9	2.5	2.7
Recovery (%)	97.8	97.2	103.4

response for paraoxon (Supplementary material, Fig. S4, curve a). Thus, the biosensor is favorably stable. Meanwhile, the long-term stability of OPH-bacteria/GCE was also tested. The current response decreased sharply during the one-month test and just remained 20% of the initial response after 1 month (Supplementary material, Fig. S4, curve b). Judging from this, the biosensor modified with OMCs was much more stable than the OPH-bacteria/GCE. It may be attributed to the uniform porous channels, large surface area and well-defined pore topology which was benefit for the immobilization of OPH-bacteria and thus improved the stability of the enzyme.

3.6. Application to real samples

To study the applicability of OPH-bacteria/OMCs/GCE, tap water, seawater and sewage were measured as the real samples. The samples were filtered through a well-defined 0.22 μm membrane. Before measurement, the ionic strength and pH of the real samples should be adjusted to match with the PBS buffer used in this study. The recovery of this method was investigated by the standard-addition method. Each of the samples was measured for six times and the average was calculated. The proposed method was applicable for the detection of real samples as all the recoveries are between 95% and 105% (Table 2).

4. Conclusions

In summary, a highly specific, sensitive and rapid microbial biosensor for *p*-nitrophenyl-substituted OPs was developed by inclusion of OMCs with OPH-bacteria prepared in our laboratory. Under the optimized experimental conditions, at OPH-bacteria/OMCs/GCE, the current response was linear with paraoxon concentration in 0.05–25 μM, linear range of 0.05–25 μM for parathion, and 0.08–30 μM for methyl parathion. The low limits of detection were evaluated to be 9.0 nM for paraoxon, 10 nM for parathion and 15 nM for methyl parathion. The proposed electrochemical microbial biosensor exhibited good operating stability and long-term stability and is well-suited for meeting the challenges of on-site determination.

Acknowledgments

This work was financially supported by National Natural Science Foundation of China (Nos. 91227116, 31200598, 31300663 and 21275152) and the Hundred-Talent-Project (No. KSCX2-YW-BR-7), Chinese Academy of Sciences.

Appendix A. Supporting information

Supplementary data associated with this article can be found in the online version at http://dx.doi.org/10.1016/j.bios.2014.04.001.

References

Ashok Mulchandani, R., 2011. Appl. Biochem. Biotechnol. 165, 687–699.
Bravo, R., Driskell Jr., W.J., Whitehead Ralph, D., Needham, L.L., Barr, D.B., 2002. J. Anal. Toxicol. 26, 245–252.
Brown, M.A., Brix, K.A., 1998. J. Appl. Toxicol. 18, 393–408.
Chen, Q., Fung, Y., 2010. Electrophoresis 31, 3107–3114.
Chen, S., Huang, J., Du, D., Li, J., Tu, H., Liu, D., Zhang, A., 2011. Biosens. Bioelectron. 26, 4320–4325.
Choi, B.G., Park, H., Park, T.J., Yang, M.H., Kim, J.S., Jang, S.-Y., Heo, N.S., Lee, S.Y., Kong, J., Hong, W.H., 2010. ACS Nano 4, 2910–2918.
Chough, S.H., Mulchandani, A., Mulchandani, P., Chen, W., Wang, J., Rogers, K.R., 2002. Electroanalysis 14, 273–276.
Deo, R.P., Wang, J., Block, I., Mulchandani, A., Joshi, K.A., Trojanowicz, M., Scholz, F., Chen, W., Lin, Y., 2005a. Anal. Chim. Acta 530, 185–189.
Deo, R.P., Wang, J., Block, I., Mulchandani, A., Joshi, K.A., Trojanowicz, M., Scholz, F., Chen, W., Lin, Y.H., 2005b. Anal. Chim. Acta 530, 185–189.
Du, D., Chen, W., Zhang, W., Liu, D., Li, H., Lin, Y., 2010. Biosens. Bioelectron. 25, 1370–1375.
Eskenazi, B., Bradman, A., Castorina, R., 1999. Environ. Health Perspect. 107, 409–419.
Fukuda, T., Tsuchiyama, K., Makishima, H., Takayama, K., Mulchandani, A., Kuroda, K., Ueda, M., Suye, S., 2010. Biotechnol. Lett. 32, 655–659.
Kassa, J., Králové, H., 2002. Clin. Toxicol. 40, 803–816.
Karami, A., Latifi, A.M., Khodi, S., 2014. J Microbiol. Biotechnol. 24, 379–385.
Laothanachareon, T., Champreda, V., Sritongkham, P., Somasundrum, M., Surareungchai, W., 2008. World J. Microbiol. Biotechnol. 24, 3049–3055.
Lee, J.H., Park, J.Y., Min, K., Cha, H.J., Choi, S.S., Yoo, Y.J., 2010. Biosens. Bioelectron. 25, 1566–1570.
Lei, C., Valenta, M.M., Saripalli, K.P., Ackerman, E.J., 2007. J. Environ. Qual. 36, 233–238.
Lei, Y., Mulchandani, P., Wang, J., Chen, W., Mulchandan, A., 2005. Environ. Sci. Technol. 39, 8853–8857.
Li, L., Liang, B., Li, F., Shi, J., Mascini, M., Lang, Q., Liu, A., 2013. Biosens. Bioelectron. 42, 156–162.
Li, L., Liang, B., Shi, J., Li, F., Mascini, M., Liu, A., 2012. Biosens. Bioelectron. 33, 100–105.
Liu, R., Yang, C., Xu, Y., Xu, P., Jiang, H., Qiao, C., 2013. J. Agric. Food Chem. 61, 7810–7816.
Lukaszewicz-Hussain, A., 2010. Pestic. Biochem. Physiol. 98, 145–150.
Mathew, S.B., Pillai, A.K., Gupta, V.K., 2007. Spectrochim. Acta Part A 67, 1430–1442.
Minton, N.A., Murray, V.S., 1988. Med. Toxicol. Adverse Drug Exp. 3, 350–375.
Mulchandani, P., Chen, W., Mulchandani, A., 2001. Environ. Sci. Technol. 35, 2562–2565.
Mulchandani, P., Chen, W., Mulchandani, A., 2006. Anal. Chim. Acta 568, 217–221.
Ndamanisha, J.C., Guo, L., 2012. Anal. Chim. Acta 747, 19–28.
Pinto, C.G., Pavh, J.L.W., Cordem, B.M., 1995. Anal. Chem. 67, 2606–2612.
Rahimi, R., Abdollahi, M., 2007. Pestic. Biochem. Physiol. 88, 115–121.
Schoning, M.J., Krause, R., Block, K., Musahmeh, M., Mulchandani, A., Wang, J., 2003. Sens. Actuators B Chem. 95, 291–296.
Schofield, D., Westwater, C., Barth, J., DiNovo, A., 2007. Appl. Biochem. Biotechnol. 76, 1383–1394.
Shimazu, M., Nguyen, A., Mulchandani, A., Chen, W., 2003. Biotechnol. Prog. 19, 1612–1614.
Soltaninejad, K., Abdollahi, M., 2009. Med. Sci. Monit. 15, 75–79.
Takayama, K., Suye, S., Tanaka, Y., Mulchandani, A., Kuroda, K., Ueda, M., 2011. Anal. Sci. 27, 823–826.
Tang, X., Liang, B., Yi, T., Giuseppe, Manco, Palchetti, I., Liu, A., 2014. Enzym. Microb. Technol. 55, 107–112.
Wang, J., Krause, R., Block, K., Musameh, M., Mulchandani, A., 2003. Biosens. Bioelectron. 18, 255–260.
Wang, J., Krause, R., Block, K., Musameh, M., Mulchandani, A., Mulchandani, P., Chen, W., 2002. Anal. Chim. Acta 469, 197–203.
Zhang, T., Lang, Q., Yang, D., Li, L., Zeng, L., Zheng, C., Li, T., Wei, M., Liu, A., 2013. Electrochim. Acta 106, 127–134.
Zhang, T., Lang, Q., Zeng, L., Li, T., Wei, M., Liu, A., 2014a. Electrochim. Acta 115, 283–289.
Zhang, T., Zeng, L., Han, L., Li, T., Zheng, C., Wei, M., Liu, A., 2014b. Anal. Chim. Acta 822, 23–29.